Residual stress characterization for cold expansion utilizing spatial statistics: The SpARS methodology

Dallen L. Andrew, Ph.D.
Hill Engineering, LLC

Presentation for:
ERSI Analysis Methods and Testing Committee
3 September 2020

Acknowledgements

- UTSA Doctoral Committee
  - Dr. Hai-Chao Han, UTSA
  - Dr. Adel Alaeddini, UTSA
  - Dr. Mark Thomsen, USAF A-10
  - Dr. Juan Ocampo, St. Mary's University
  - Dr. Carl Popelar, Southwest Research Institute
- United States Air Force
  - A-10 ASIP, T-38 ASIP
- Hill Engineering
- Southwest Research Institute
- Many others
  - Josh Hodges (BAMF)
  - Dr. Tom Mills (APES)
  - Dr. Scott Carlson (Lockheed Martin)

UTSA The University of Texas at San Antonio

U.S. AIR FORCE

SwRI SOUTHWEST RESEARCH INSTITUTE

HILL ENGINEERING
Predict. Test. Perform.

Outline

- Introduction
  - Motivation, Objective
- Experimental Data Overview
- Part 1: Spatial Analysis of Residual Stress
  - Methods
    - Kriging, Bootstrapping, Statistical Characterization
  - Results
    - Comparison to test data, Numerical verification
- Part 2: Fatigue Crack Growth Analysis
  - Methods
    - Simulation process (BAMF, FEA, FCG)
  - Results
    - Comparison to test data
  - Summary
- Conclusions
- Future Work

INTRODUCTION

Motivation

- Current approved analysis methods for using residual stress (RS) from cold expansion (Cx) for aircraft are non-existent or are rudimentary
  - Widely used but analysis tool lag behind
- Reduced initial crack size approach has many limitations:
  - Not physics-based
  - Does not account for crack growth shape, interactions between the RS field and other geometric features (holes, edges), or the 3D stress state from Cx (entrance vs. exit side)
  - Very limited benefit in aircraft sustainment for recurring inspection interval
  - Shown to be unconservative in some situations
  - Does not use standard allowable-based approach frequently used in static analyses of aerospace structures

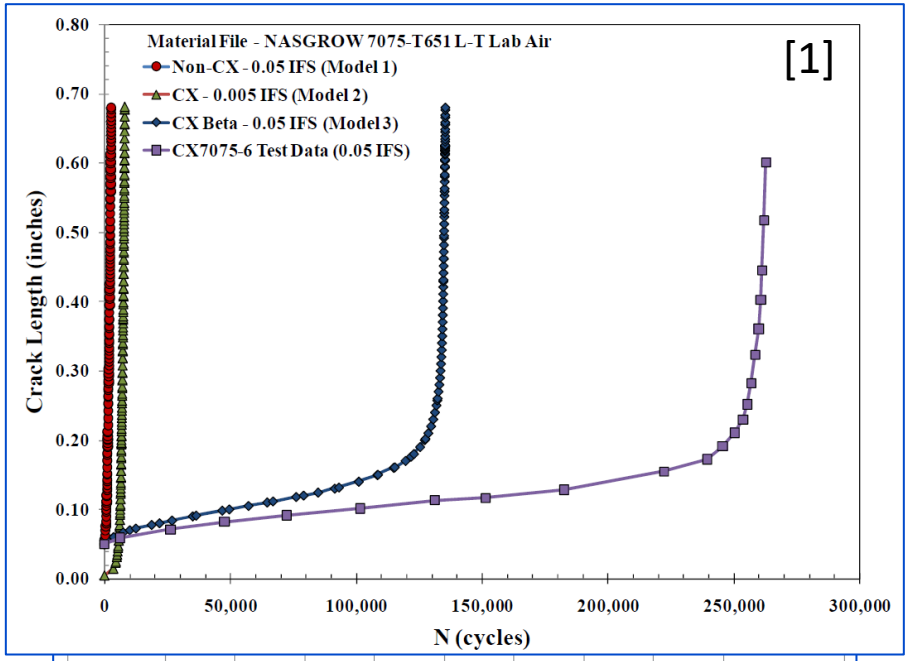

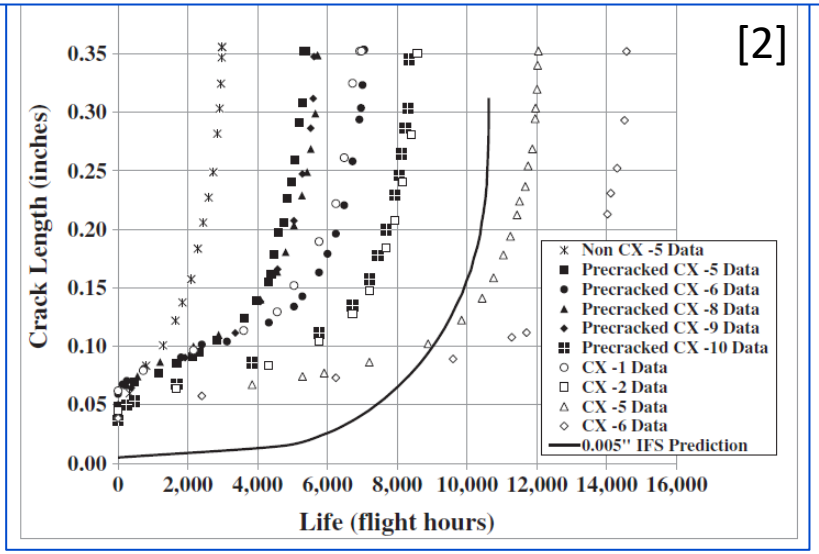

Objective

Develop a process to statistically quantify residual stress fields from Cx utilizing spatial statistical methods and identify impact on fatigue life

- Approach:
  - Statistically characterize residual stress fields from Cx using spatial statistical methods
  - Use these statistically defined residual stress fields in deterministic fatigue crack growth analyses
  - Compare results to existing experimental data (residual stress and fatigue)
- Outcome:
  - Establish mature standard methodology for using residual stress for crack growth analyses

EXPERIMENTAL DATA OVERVIEW

Experimental Data

- Existing RS and fatigue crack growth test data from Cx holes
  - Used in recent round robin evaluations by the Engineered Residual Stress Implementation (ERSI) working group
- Details
  - Material = 2024-T351
  - Geometry = 4 inch wide, 0.25 inch thick, 0.5 inch diameter, center and offset hole
  - FTI 16-0-N tool kit, mean and minimum applied expansion
- Three conditions with multiple replicates
  - A2 condition (RS replicates = 5, fatigue replicates = 2)
    - Center hole, min applied expansion (~3.2%)
  - E1 condition (RS replicates = 5, fatigue replicates = 9)
    - Center hole, mean applied expansion (~3.7%)
  - B1 condition (RS replicates = 4, fatigue replicates = 4)
    - Offset hole (0.6 inch), min applied expansion (~3.2%)

$$\mathrm{I}_a = \frac{(D_m + 2t_{ss} - D) \cdot 100\%}{D}$$

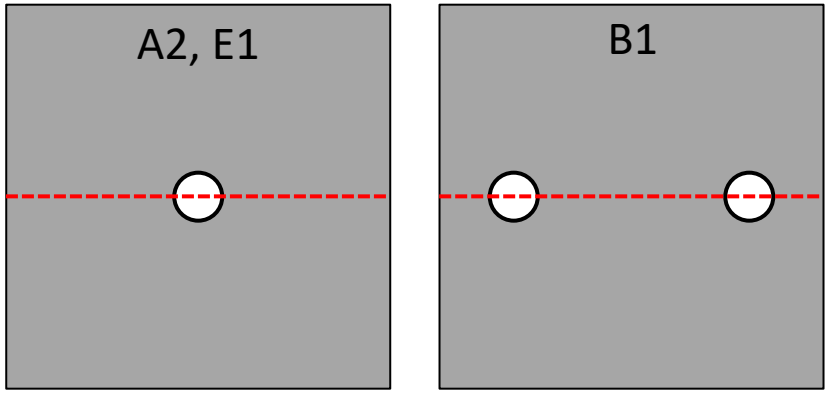

Methods

PART 1: SPATIAL ANALYSIS OF RESIDUAL STRESS

Spatial Analysis of Residual Stress

- Overview

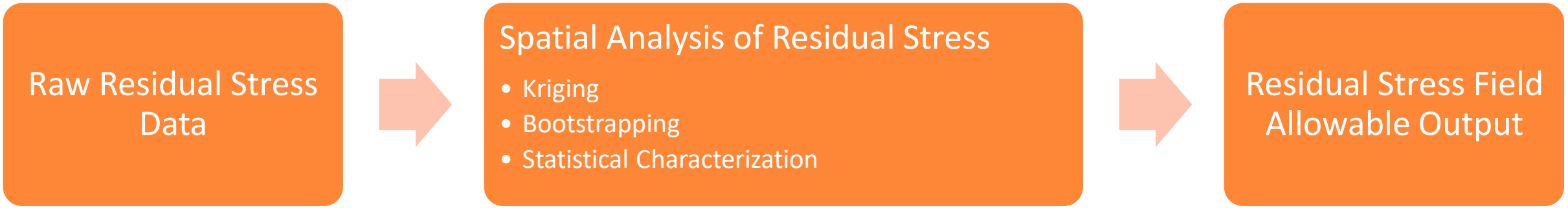

Tobler's 1st Law of Geography [3]:

"Everything is related to everything else, but near things are more related than distant things."

Kriging

- Kriging: An advanced geostatistical procedure that generates an estimated response surface from a scattered set of points
  - Assumes distance between sample points reflects spatial correlation that explain variation in the surface
  - Unlike other interpolation methods, kriging is a geostatistical interpolation method that includes autocorrelation (the statistical relationships among the measured points)
  - Raw residual stress data was used as the training points for the model
  - The Gaussian correlation function was selected & provided least error
  - Distances between all points to all other points are then correlated
- Used to regress the multiple replicate coupons observations
  - Subsampling algorithm applied to reduce number of training points actually used as inputs, as the calculations triple the order of magnitude of the correlation matrix
  - ~34,000 points/replicate*5 replicates = 170,000 x 170,000 point matrix ^3 = 4.9e15x4.9e15 point matrix

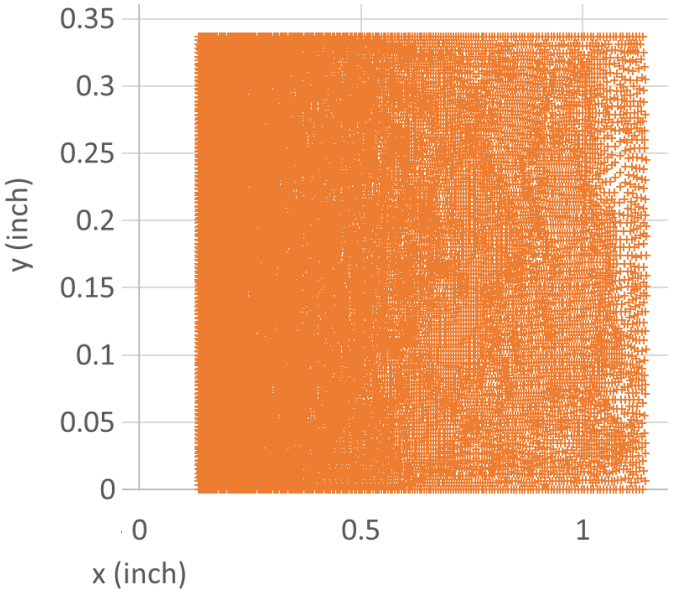

Bootstrapping

- Bootstrapping: Resampling technique that allows uncertainty quantification through construction of statistical distributions
  - No assumption is made on the underlying distribution of replicate samples
  - Estimates population distribution at each (x,y) coordinate by repeatedly obtaining samples with replacement from the Kriging model
  - Done in two steps/loops
    - First (inner) loop samples Kriging model N times and ranks the values
    - Second (outer) loop repeats inner loop M times for a total of NxM samples

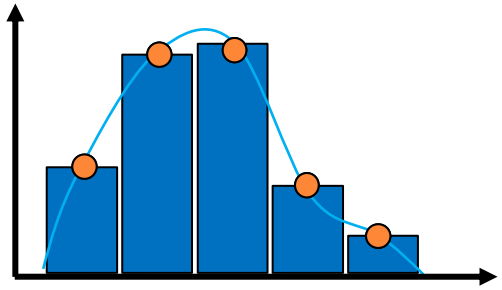

Original 5 replicate samples

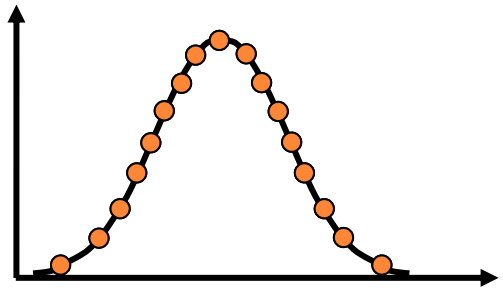

Sample N times and rank

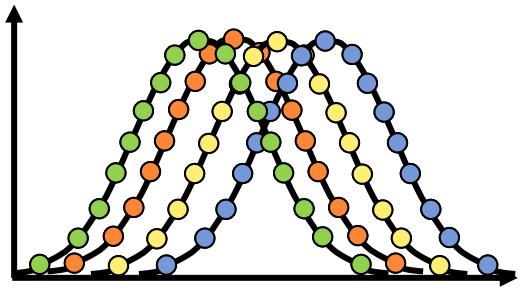

Make NxM samples

Statistical Characterization

- A process of Kriging and bootstrapping was used to statistically characterize RS field
  - Developed tolerance bounds that contain certain proportion of the population with specified level of confidence following A-basis and B-basis methods for static strength allowable values in aircraft industry
  - A-basis: at least 99% of the population equals or exceeds the value with 95% confidence
  - B-basis: at least 90% of the population equals or exceeds the value with 95% confidence

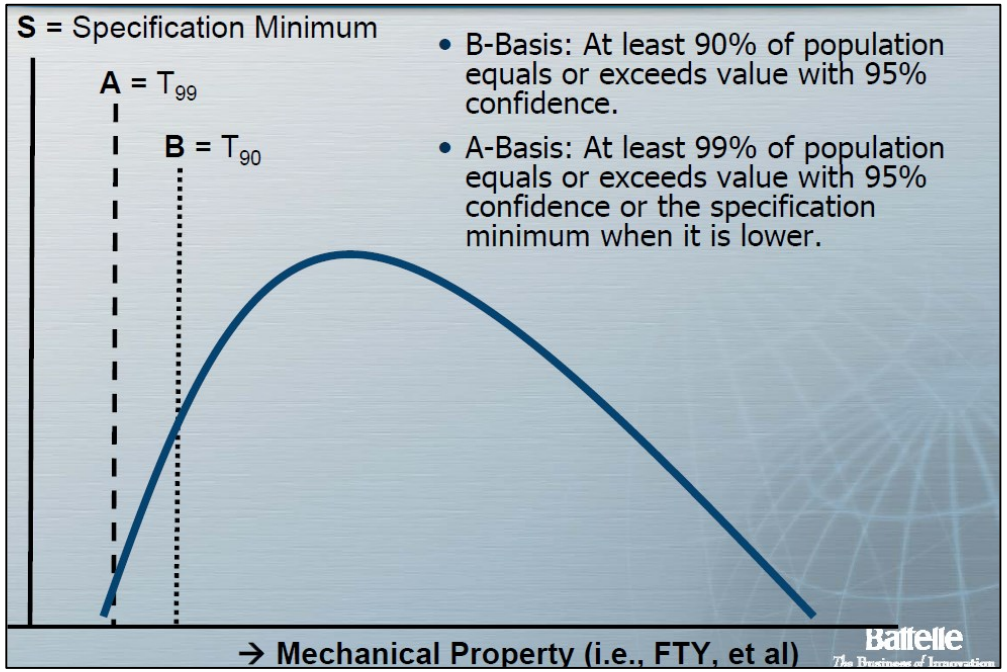

[4]

Statistical Characterization

- Define residual stress tolerance bounds as $RS_{x/y}$
  - x% population percentile with y% confidence
  - First number refers to population percentile, where x% of population equals or is below the RS value (one sided)
  - Second number refers to confidence interval defined by upper and lower confidence limit (two sided)
    - 'U' is upper confidence limit and 'L' is lower confidence limit
- Residual stress A-basis and B-basis values
  - $RS_{99/95U}$ and $RS_{90/95U}$
- Other population percentiles and confidence limits computed
  - Example: RS_{50} (Mean)
    - 50% population percentile without a confidence interval
  - Example: $RS_{01/95L}$ (Lower tolerance bound)
    - 1% population percentile with a 95% lower confidence limit

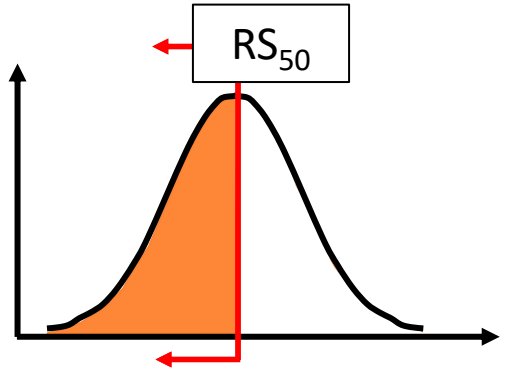

50% of population is ≤ RS_{50}

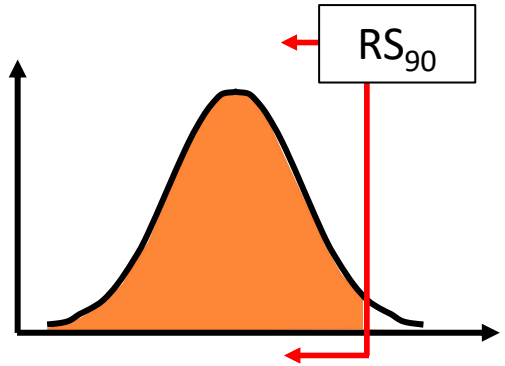

90% of population is ≤ RS_{90}

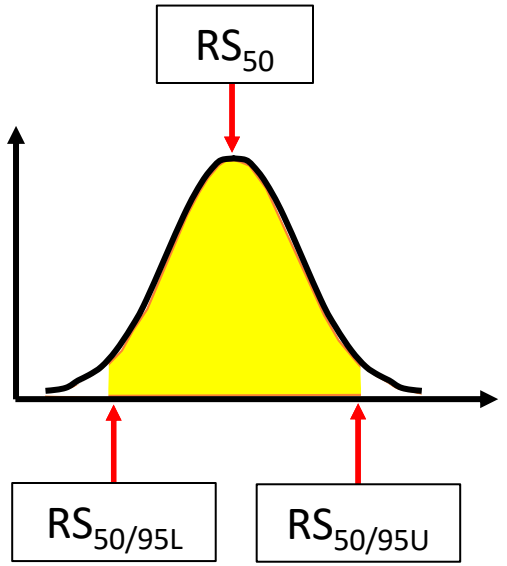

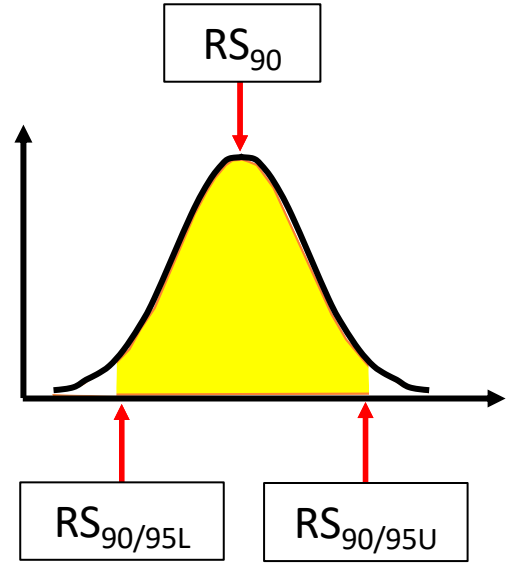

Statistical Characterization

- Using bootstrap results
- x% population percentile selected (90% in this example)
  - Bootstrap results ranked
  - Confidence interval calculated
- Accomplished using pointwise approach
  - $RS_{x/y}$ surface compiled pointwise from values at all individual points

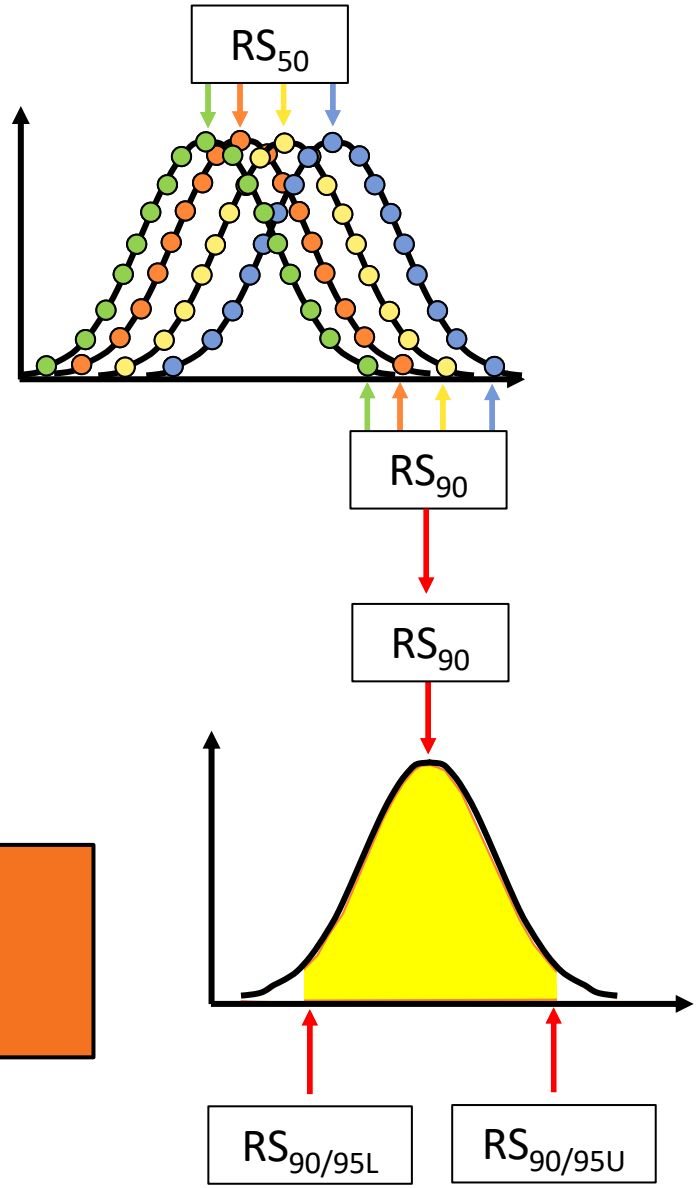

Entire process is the Spatial Analysis of Residual Stress (SpARS) method

Results

PART 1: SPATIAL ANALYSIS OF RESIDUAL STRESS

Results

- SpARS methodology was applied to A2, E1, B1 conditions

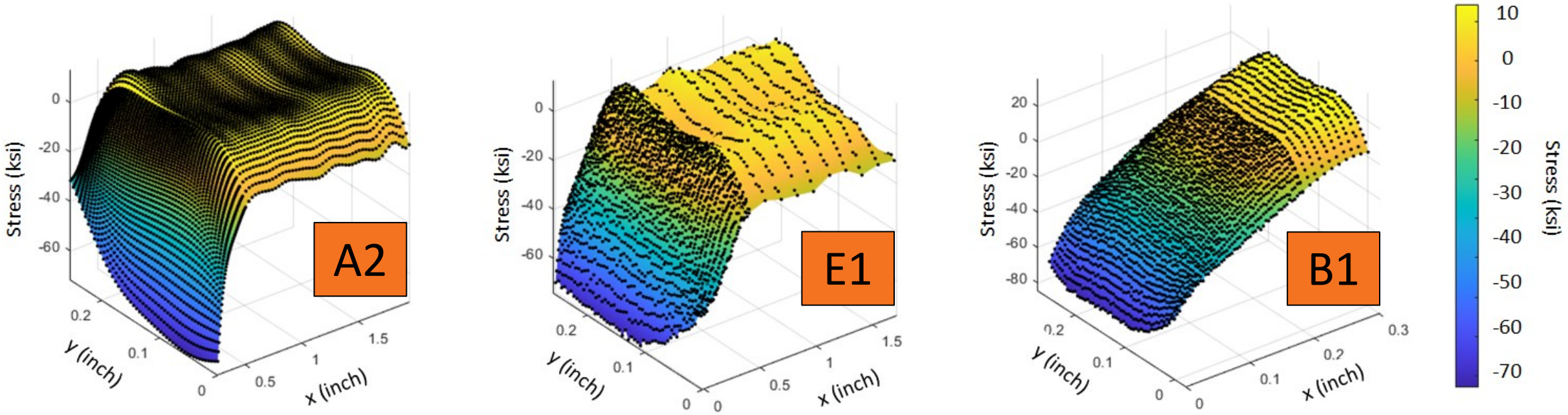

[5]

Results

- A2 RS_{50} along mid-thickness line
  - 95% confidence interval (gray), training points (black)
- Pointwise upper and lower tolerance bound surfaces obtained from the SpARS method demonstrated high spatial variability
- Used additional Kriging models as interpolators
  - Smoothed surfaces facilitate use in crack growth analysis
- Is noted that the tolerance bound RS fields are a statistical representation
  - Are not developed to meet static equilibrium
  - Area for future work

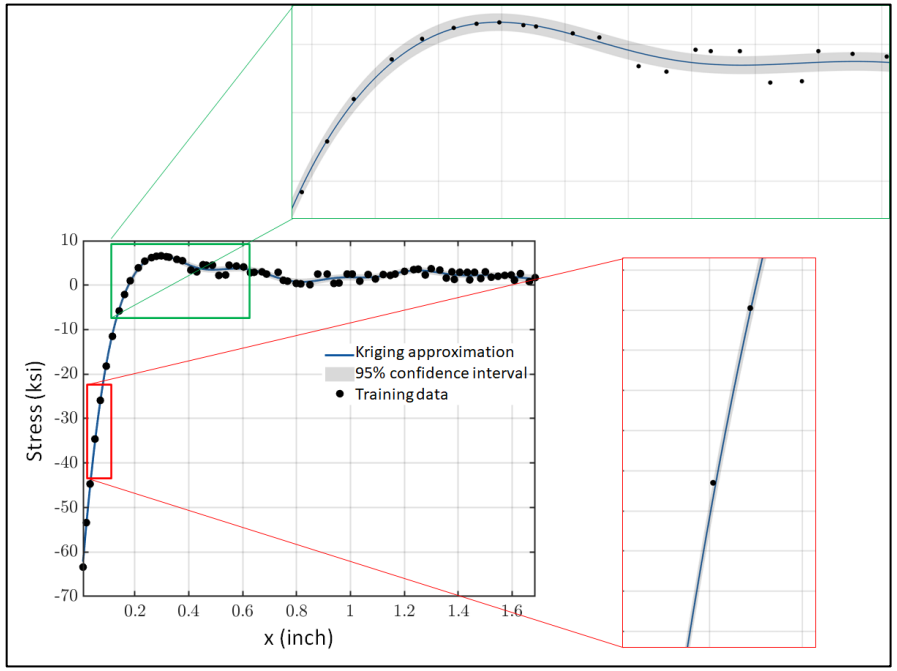

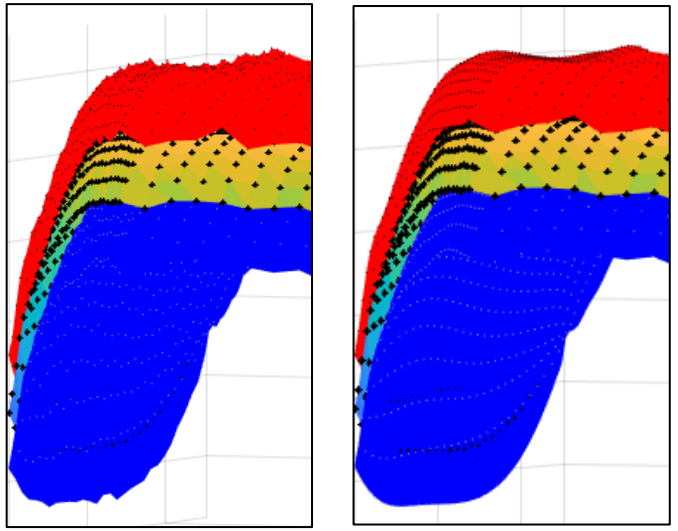

$RS_{50/95U}$

$RS_{50/95L}$

[5]

Results

- Leave-one-out (LOO) cross-validation (CV) errors
  - A2 = 2.7e-3, E1 = 1.02e-4, B1 = 4.38e-3
- Pointwise residuals on the mean between training data and SpARS
  - A2: all <3 ksi, mean = 0.14 ksi, std dev = 0.1 ksi
  - E1: all <2.5 ksi, mean = 0.68 ksi, std dev = 0.53 ksi
  - B1: all <1.5 ksi, mean = 0.46 ksi, std dev = 0.36 ksi

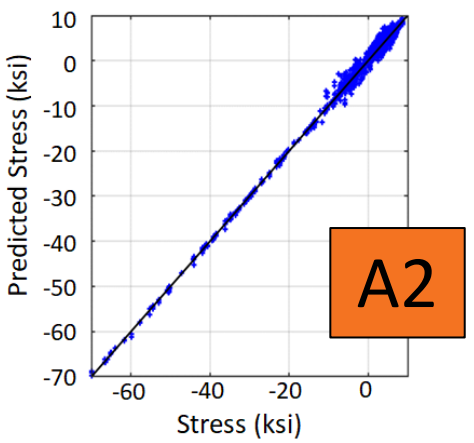

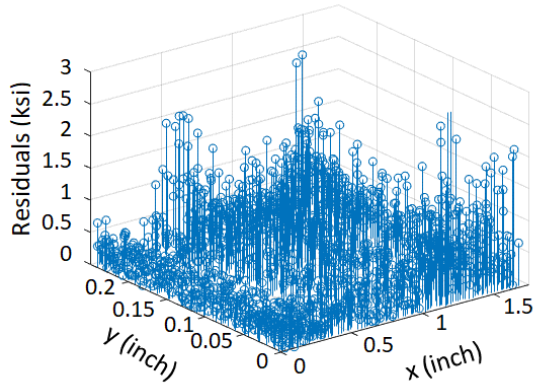

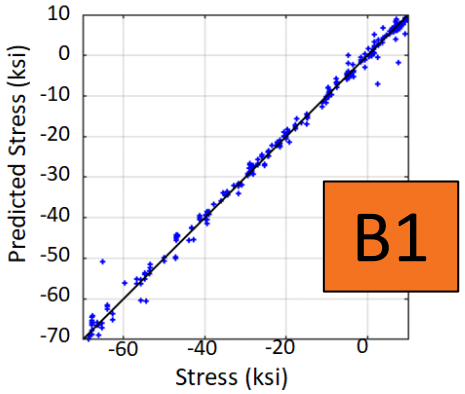

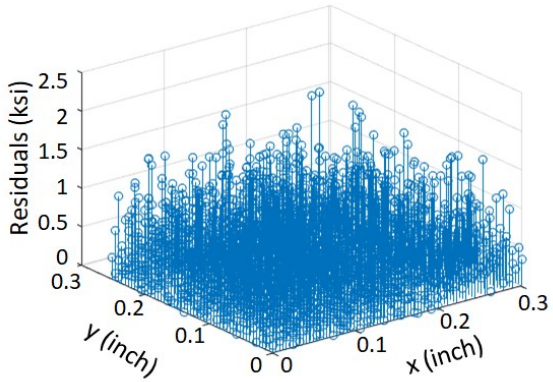

[5]

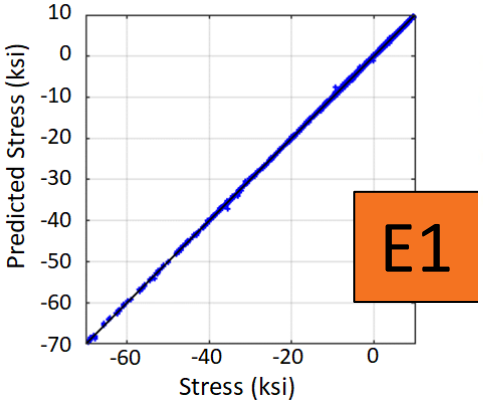

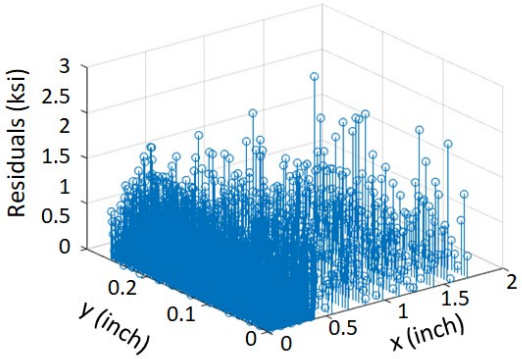

Results

- Upper and lower tolerance bounds
  - $RS_{99/95U}$ (gray mesh)
  - $RS_{01/95L}$ (pink mesh)
- Contour plots of mean, upper tolerance bound $RS_{99/95U}$ and lower tolerance bound $RS_{01/95L}$ fields

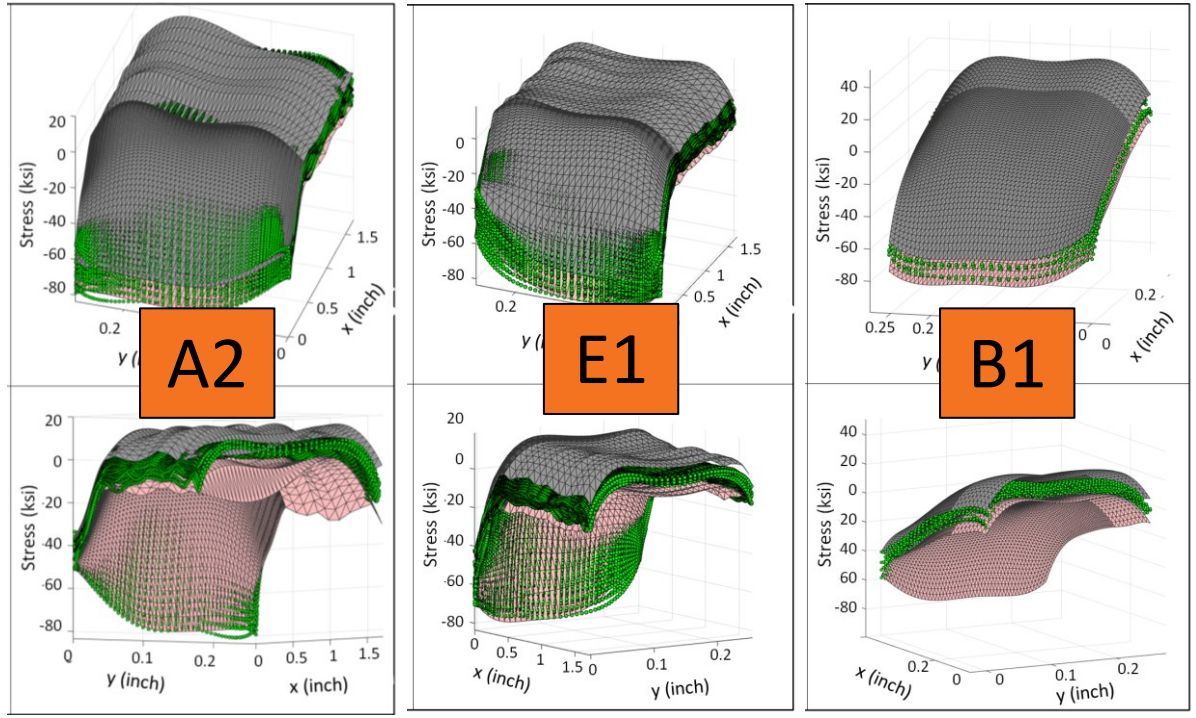

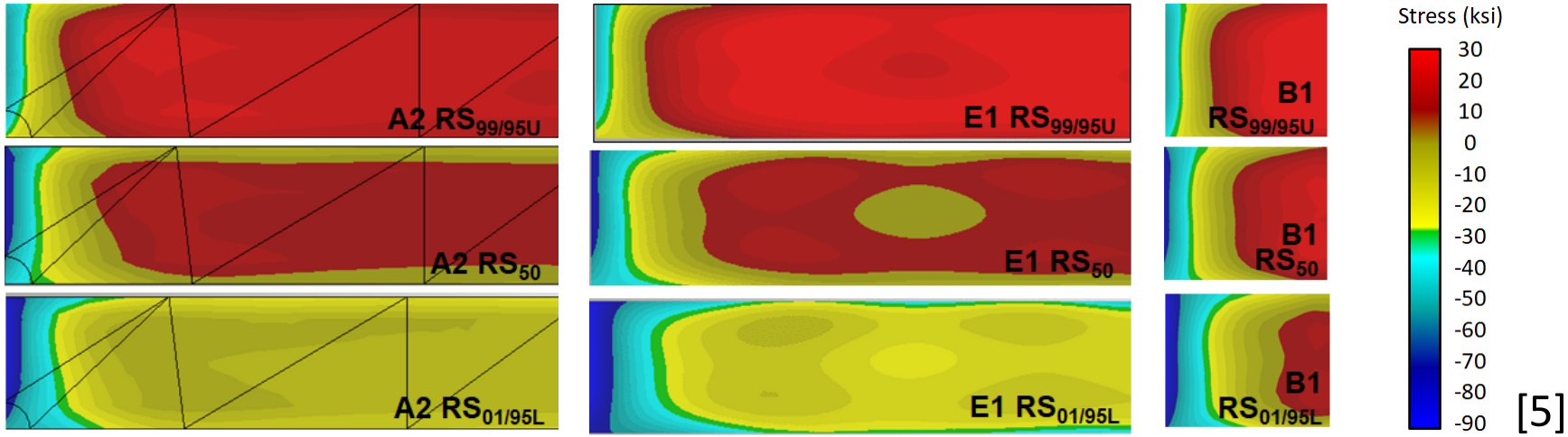

[5]

Numerical Verification

- Verification via Cx process simulation by Fatigue Technology Inc. (FTI)
  - Data consists of 29 different simulations varying six different parameters
    - Sleeve thickness, initial hole D, mandrel D elongation, yield strength, ultimate strength
    - Varied only within the allowable tolerances
  - Verification process included randomly separating training (80%) and validation (20%) data 10 different times with a response surface model for each
- Case 1
  - 1 single process simulation of fixed, known, repeatable condition (no variability)
- Case 2
  - All 29 process simulations with variation correlated solely to simulation parameters (known variability)

Numerical Verification

- Case 1: Single process simulation
  - Mean LOO CV error of 10 replicates was 9.9e-05
  - Mean validation error of 10 replicates was 1.19e-04
  - Residuals between sample mean and bootstrapped mean was low
    - Nearly all residuals <0.2 ksi, mean = 0.06 ksi

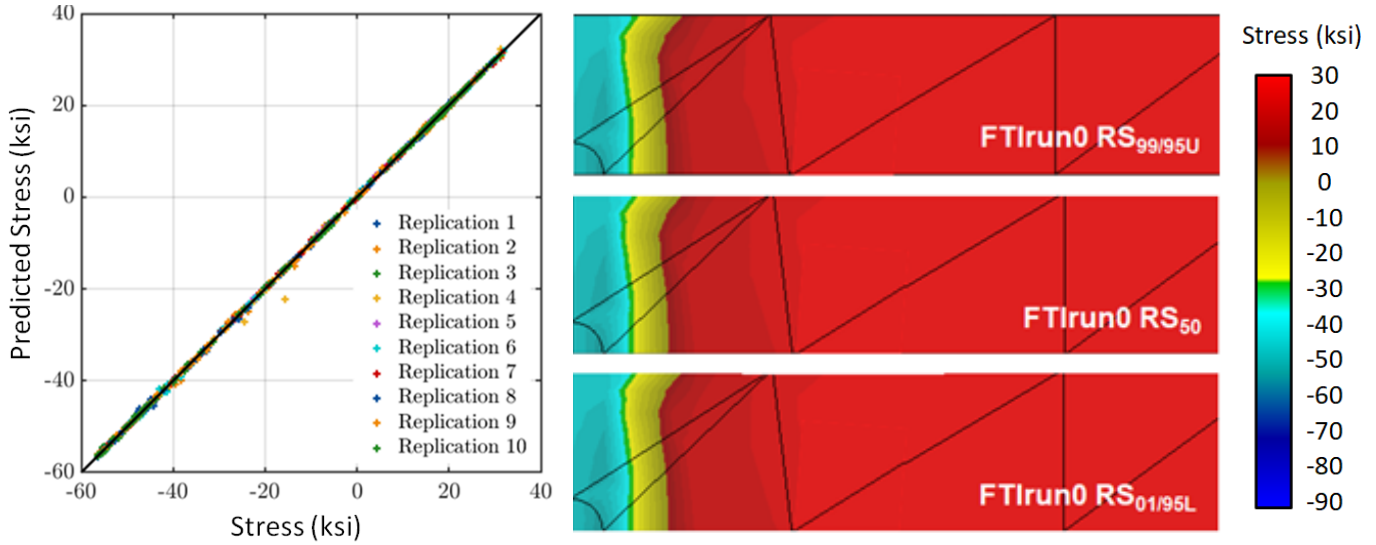

[5]

Numerical Verification

- Case 2: All 29 process simulations
  - Mean LOO CV error of 10 replicates was 9.16e-04
  - Mean validation error of 10 replicates was 1.08e-03
  - $RS_{99/95U}$ upper tolerance bound surface (gray)
  - $RS_{01/95L}$ lower tolerance bound surface (pink)

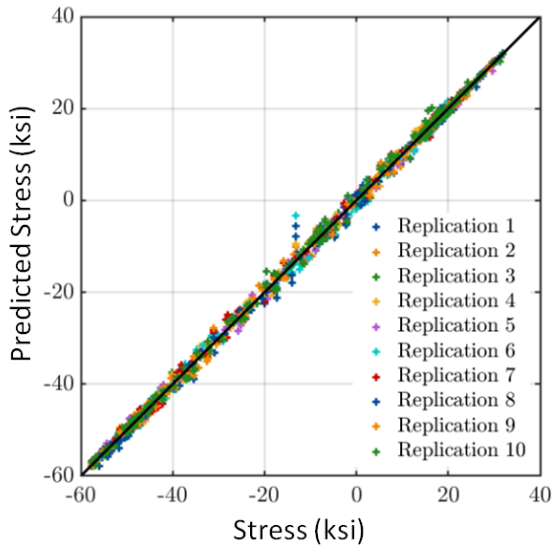

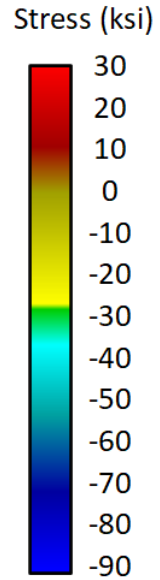

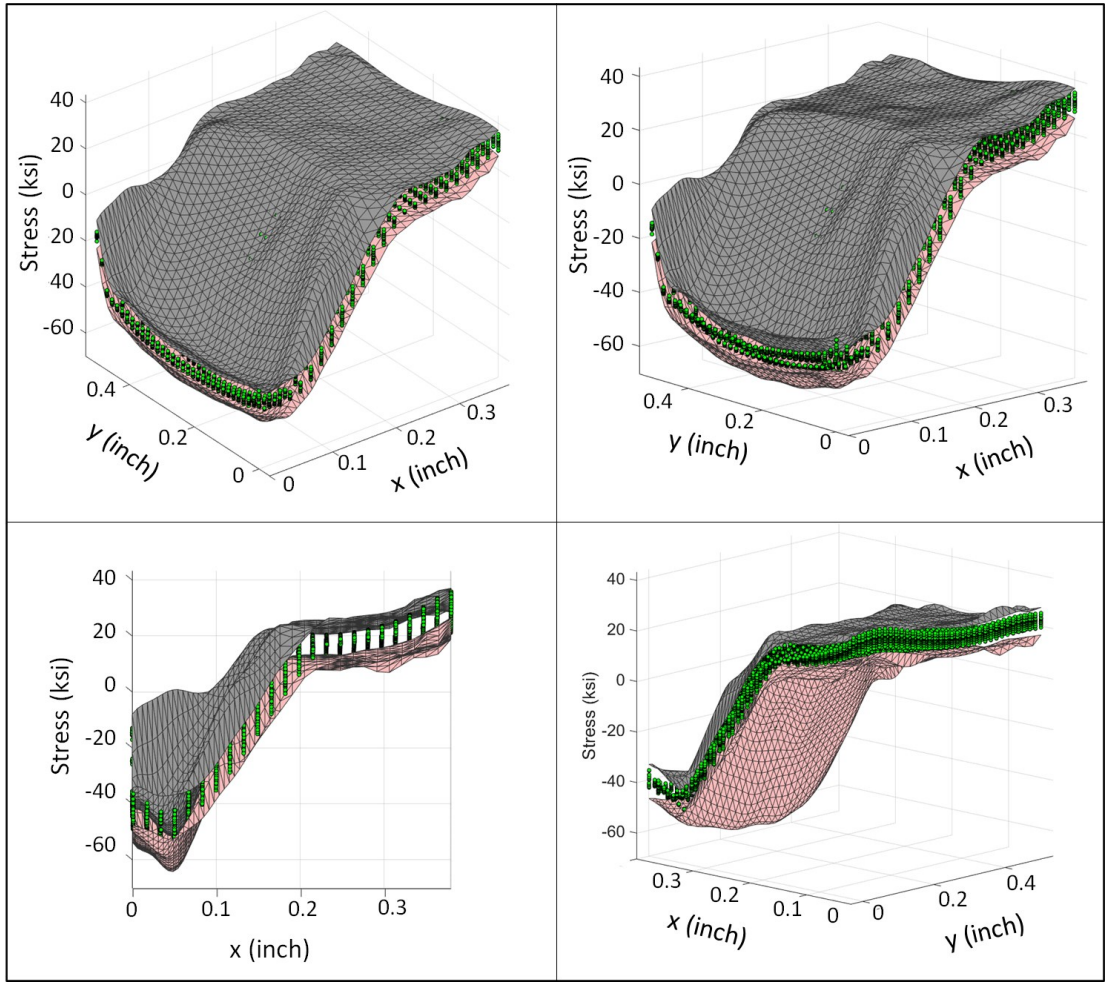

[5]

Methods

PART 2: FATIGUE CRACK GROWTH ANALYSIS

Overview

- Fatigue crack growth (FCG) analyses incorporated RS directly
- Combined multi-point stress intensity solutions from finite element analysis (FEA) with crack growth analysis
  - Physics-based crack shape evolution from actual stress state of RS field and applied loading
  - Removes analysis assumptions such as elliptical crack shapes or aspect ratio constraints
- Coupled FEA-FCG analysis implemented in Broad Application of Modeling Failure (BAMF) software
  - Stress intensity solutions from StressCheck
  - Crack growth solutions from AFGROW

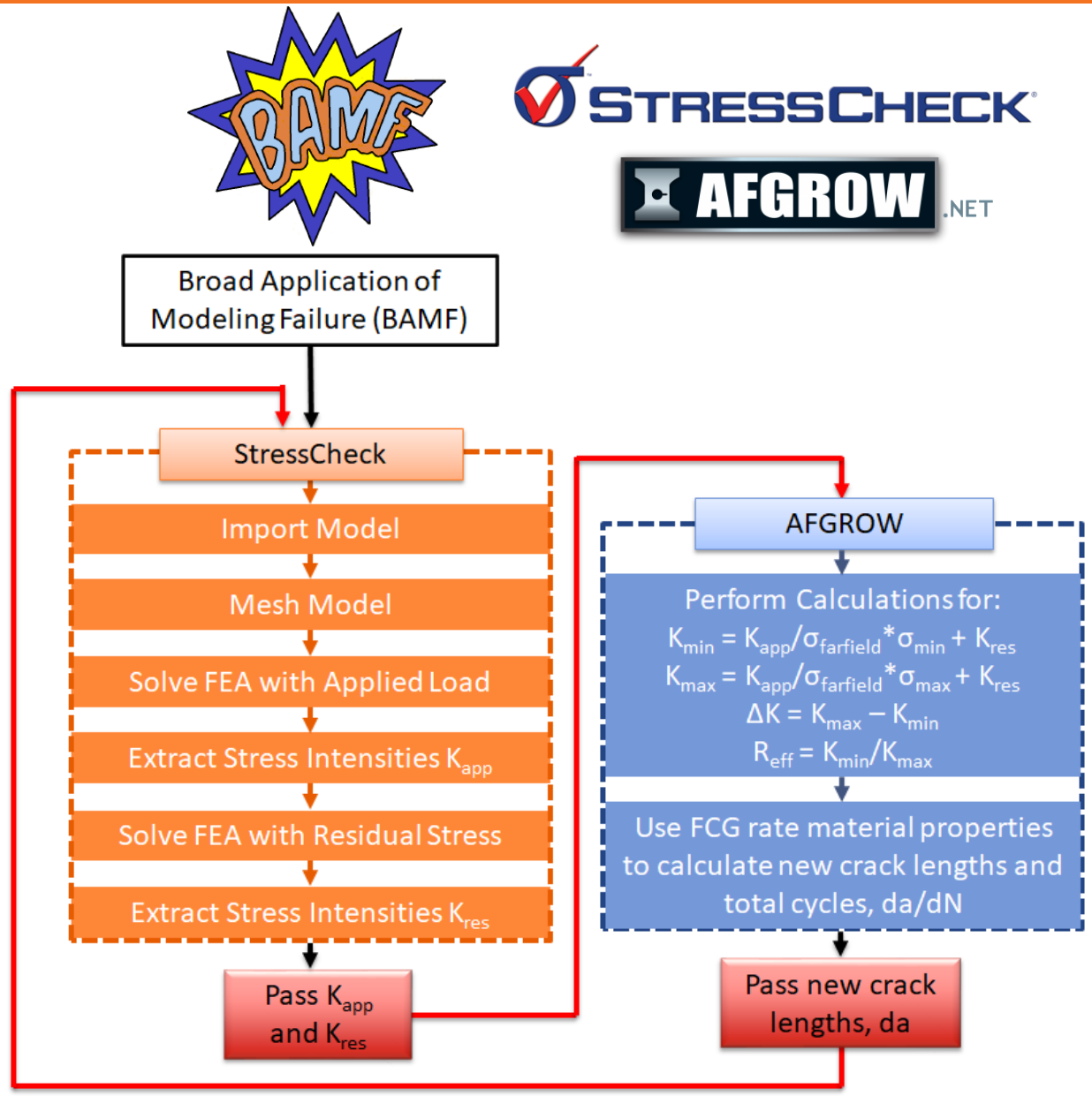

FEA

- Same dimensions as experimental coupons
- Initial crack shape (~0.05 inch corner crack) defined by a spline through 21 equally spaced points along crack front
- Crack front shape adjusts throughout analysis
  - Governed by FCG of the individual points along the crack front

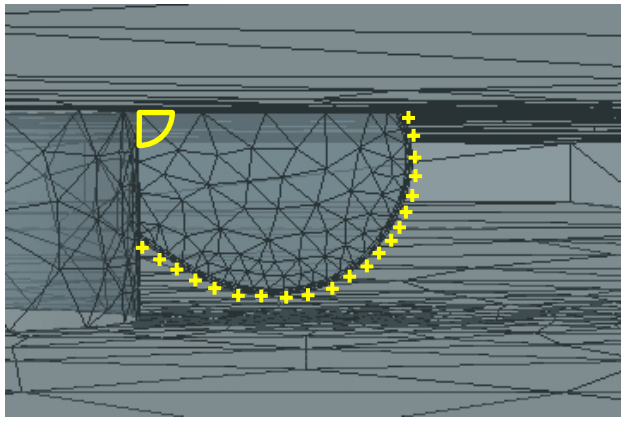

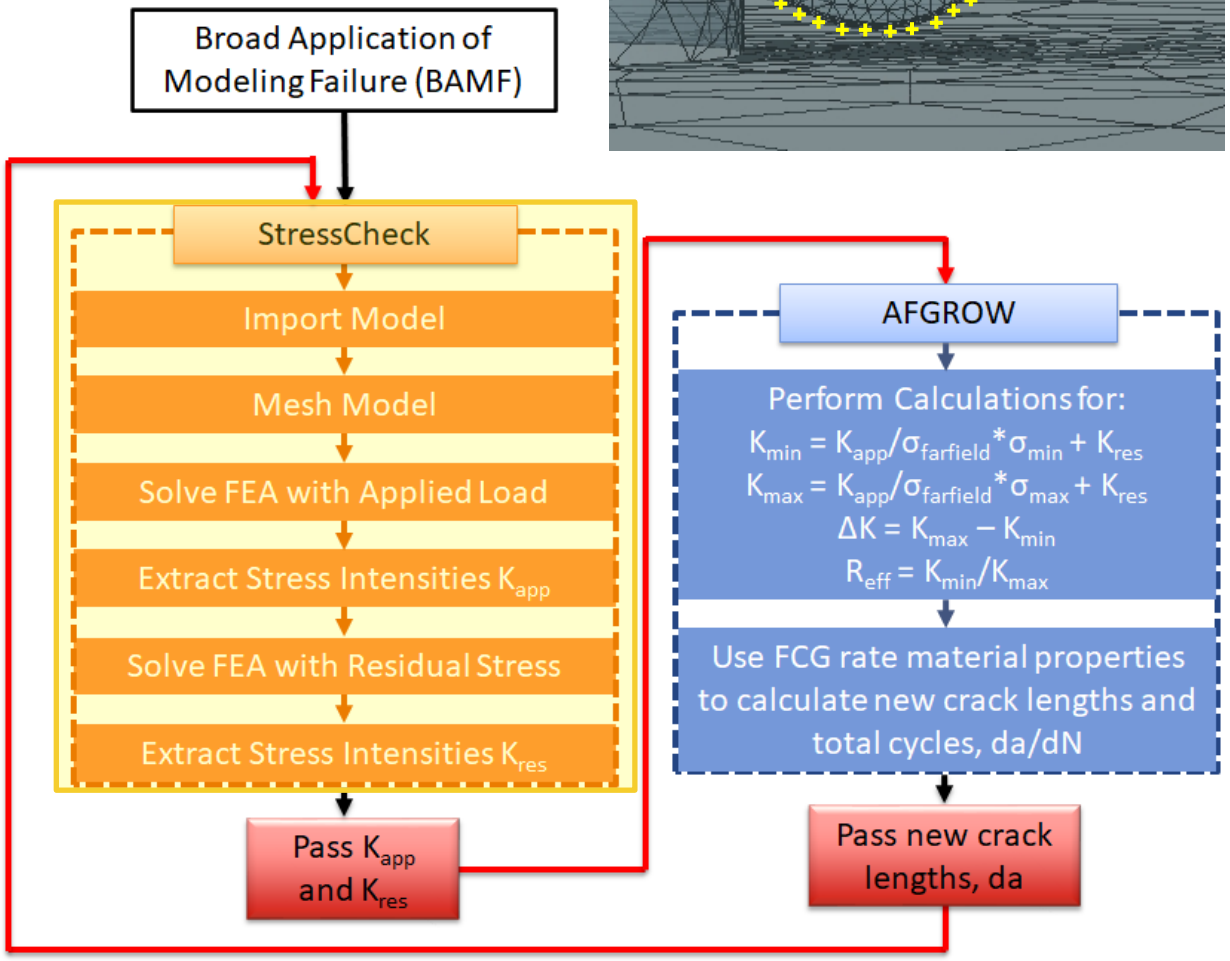

FEA

- Applied Loading
  - 25 kip applied axially at one end to match test
- Residual Stress
  - Fitting: Tabular RS data used to create 15th order polynomial function
  - Application: Polynomial function applied as normal traction load on crack face
    - Approximation that assumes RS field is static throughout the analysis and does not maintain equilibrium as crack grows
- Solving
  - K_{app} and K_{res} computed independently at each point then passed to the FCG software

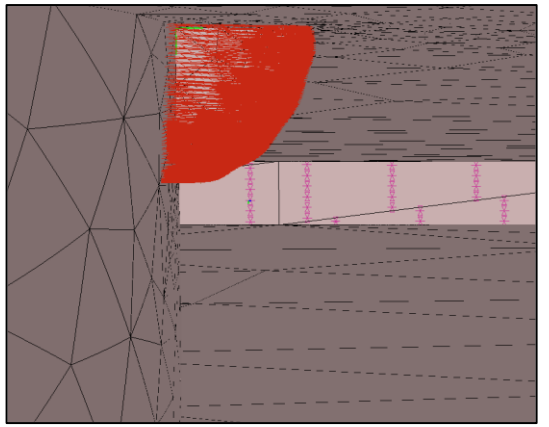

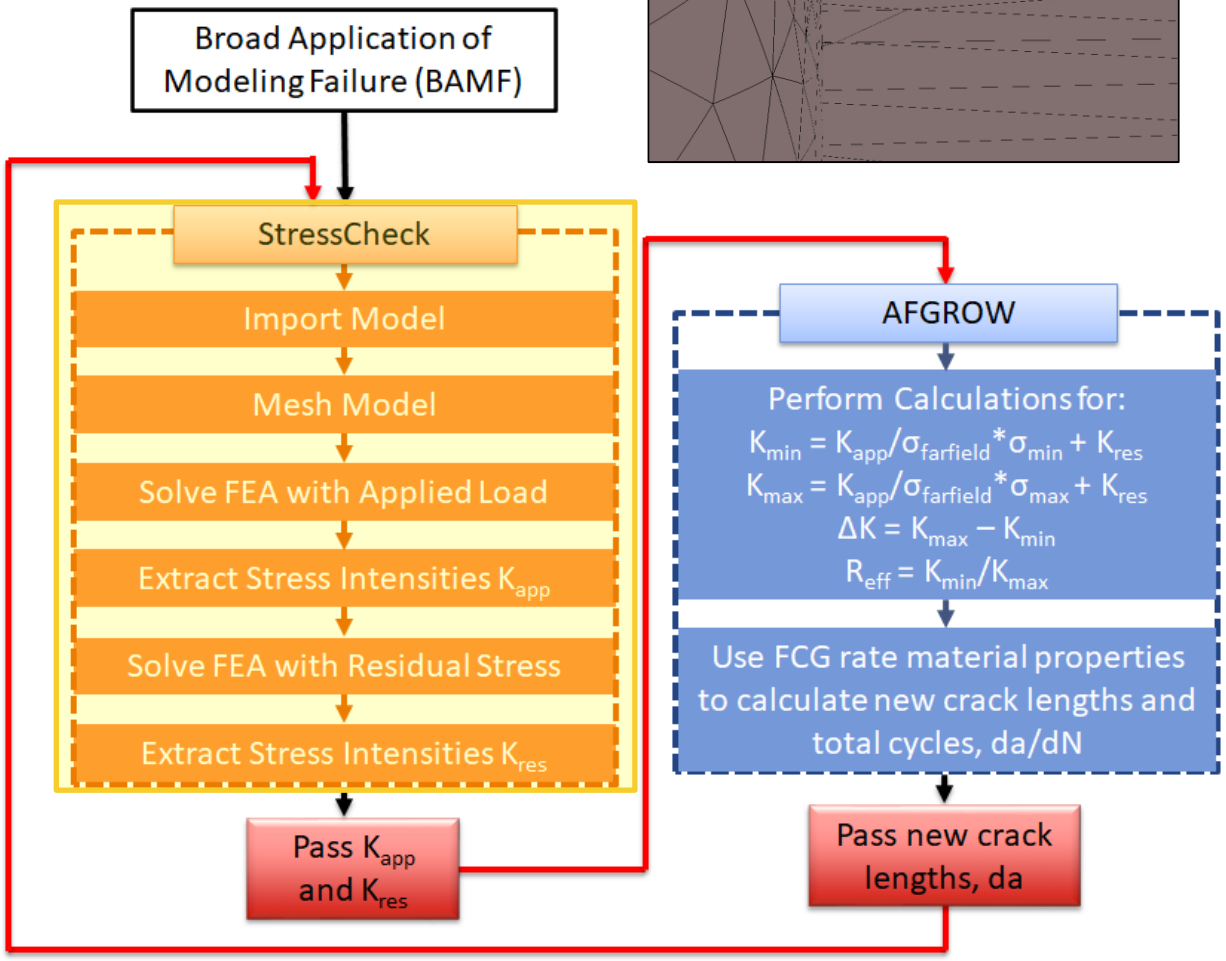

FCG

- Superposition of K_{res} and K_{app} used to incorporate total K in crack propagation algorithm
- K_{max}, K_{min}, $\Delta K = (K_{max} - K_{min})$, stress ratio (R) calculated to get da/dN using FCG rate data
- Assumptions
  - Direction of crack growth is normal to crack front
  - Crack growth (Mode I only) remains within the plane of the initially modeled crack

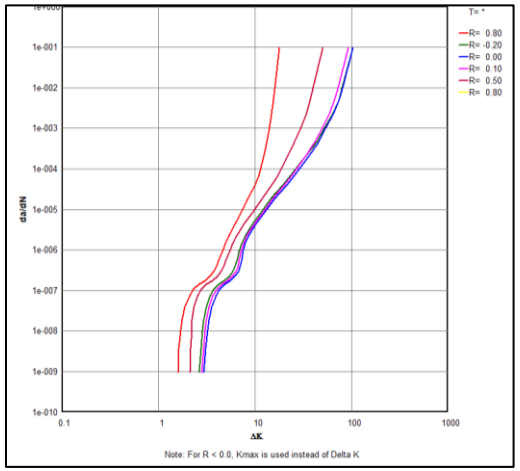

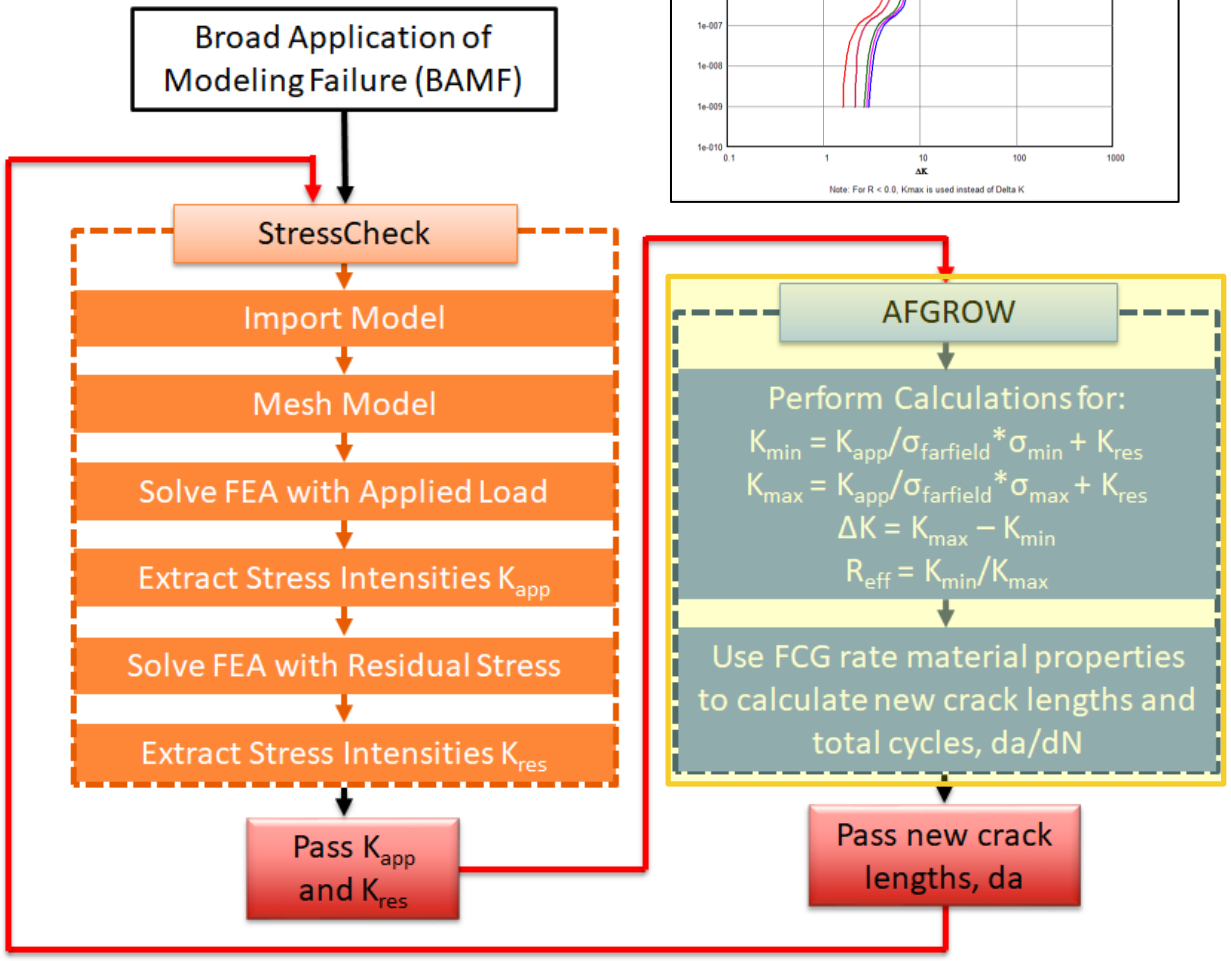

Results

PART 2: FATIGUE CRACK GROWTH ANALYSIS

FCG

- Fatigue life = Number of loading cycles from the initial crack size to failure
- Recurring inspection interval (RII) = 1/3 life from the detectable crack size to failure
  - Detectable crack size used was 0.05 inch
- Fatigue life predictions and RII of SpARS RS fields compared to ERSI test data for A2, E1, B1
  - Fatigue life and RII normalized to non-Cx case for each condition
  - Results represent effects of the RS distribution and does not address variability of the FCG test data

FCG

- A2 condition

	Fatigue Life (normalized)	RII (normalized)
Non-Cx Test Data	1.0	1.0
Cx Test Data (2 reps)	25.0-25.4	22.3-22.7
0.005 inch prediction	3.5	1.6
SpARS A2 $RS_{99/95U}$	2.9	2.9
SpARS A2 $RS_{90/95U}$	6.8	6.8
SpARS A2 RS_{90}	8.0	8.0
SpARS A2 $RS_{50/95U}$	19.9	19.9
SpARS A2 RS_{50}	28.4	28.4
SpARS A2 $RS_{50/95L}$	39.1	39.1
SpARS A2 $RS_{01/95L}$	48.6	48.6

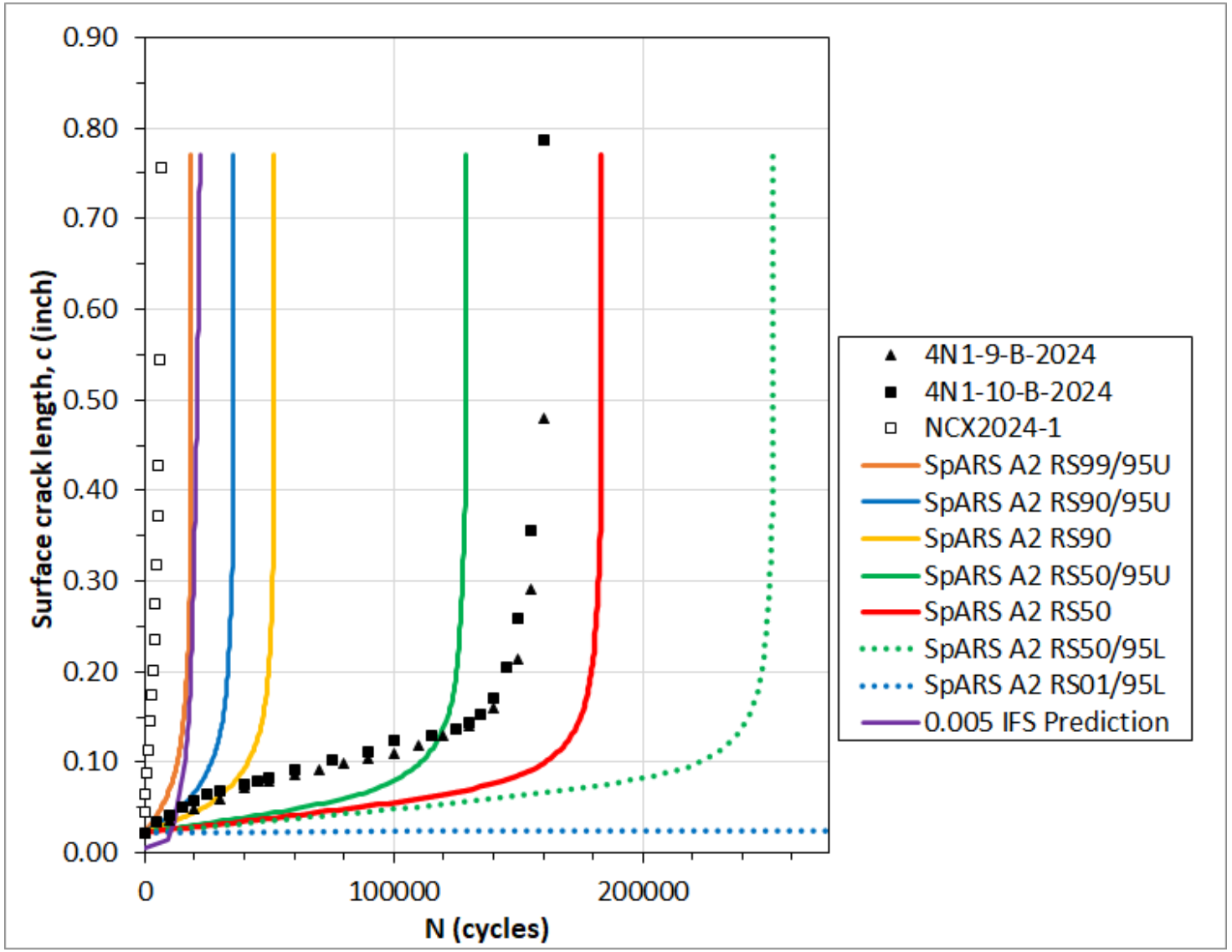

FCG

- E1 condition

Name	Fatigue Life (normalized)	RII (normalized)
Non-Cx Test Data	1.0	1.0
Cx Test Data (9 reps)	62.6-99.1	62.6-99.1
0.005 inch prediction	3.5	1.6
SpARS E1 $RS_{99/95U}$	1.2	1.2
SpARS E1 $RS_{90/95U}$	3.2	3.2
SpARS E1 RS_{90}	6.8	6.8
SpARS E1 $RS_{50/95U}$	16.1	16.1
SpARS E1 RS_{50}	39.9	39.9
SpARS E1 $RS_{50/95L}$	77.1	77.1
*SpARS E1 RS_{10}	222.2	222.2

*Note: The lower tolerance bound of $RS_{01/95L}$ resulted in no predicted FCG life, so the population and confidence limits were iteratively reduced to RS_{10} in order for the FCG analysis to run.

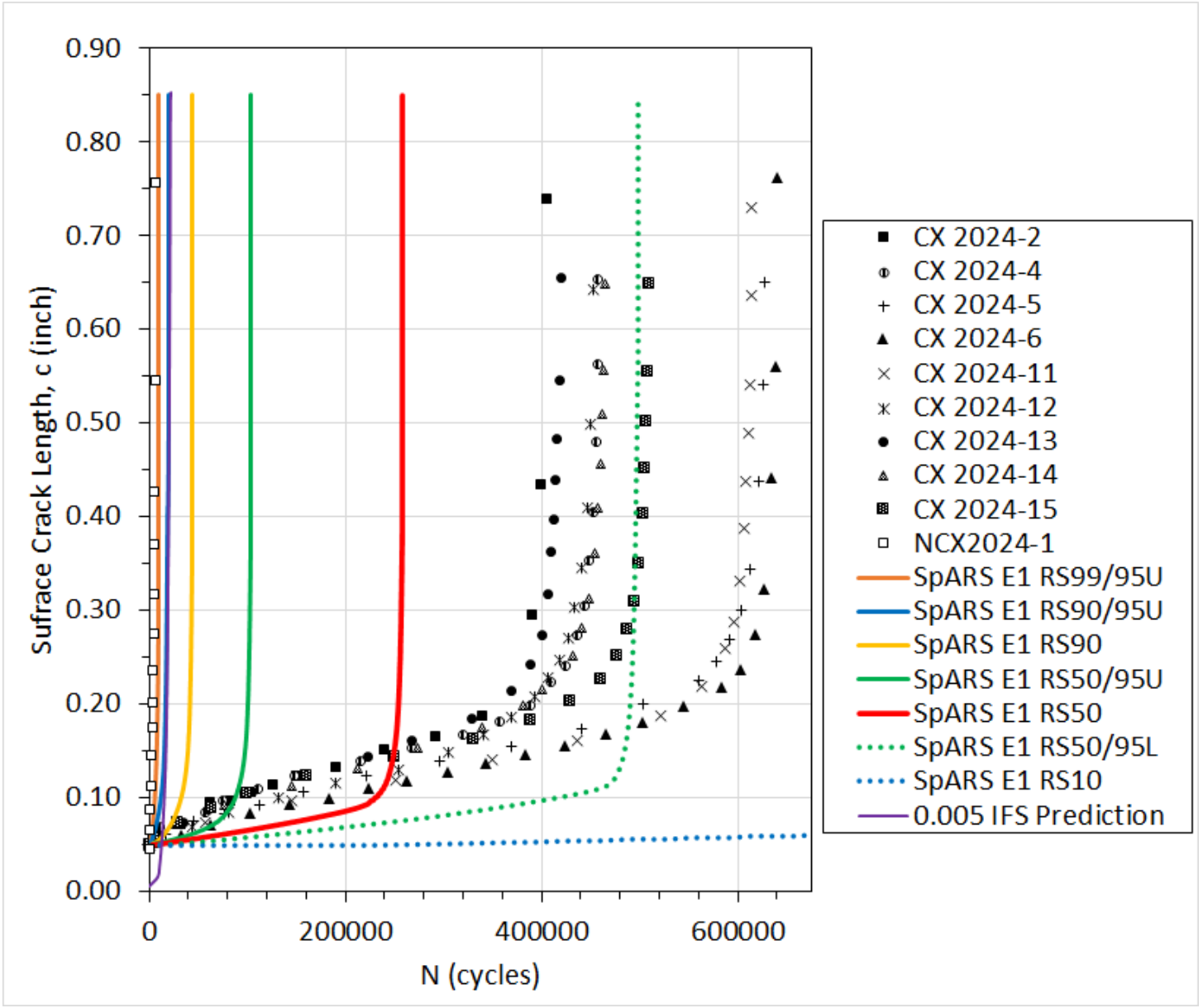

FCG

- B1 condition

Name	Fatigue Life (normalized)	RII (normalized)
Non-Cx Test Data	1.0	1.0
Cx Test Data (4 reps)	3.3-11.4	3.3-11.4
0.005 inch prediction	2.8	0.99
SpARS B1 $RS_{99/95U}$	1.3	1.3
SpARS B1 $RS_{90/95U}$	2.3	2.3
SpARS B1 RS_{90}	3.2	3.2
SpARS B1 $RS_{50/95U}$	3.7	3.7
SpARS B1 RS_{50}	5.2	5.2
SpARS B1 $RS_{50/95L}$	8.2	8.2
*SpARS B1 $RS_{10/95L}$	37.3	37.3

*Note: The lower tolerance bound of $RS_{01/95L}$ resulted in no predicted FCG life, so the population and confidence limits were iteratively reduced to $RS_{10/95L}$ in order for the FCG analysis to run.

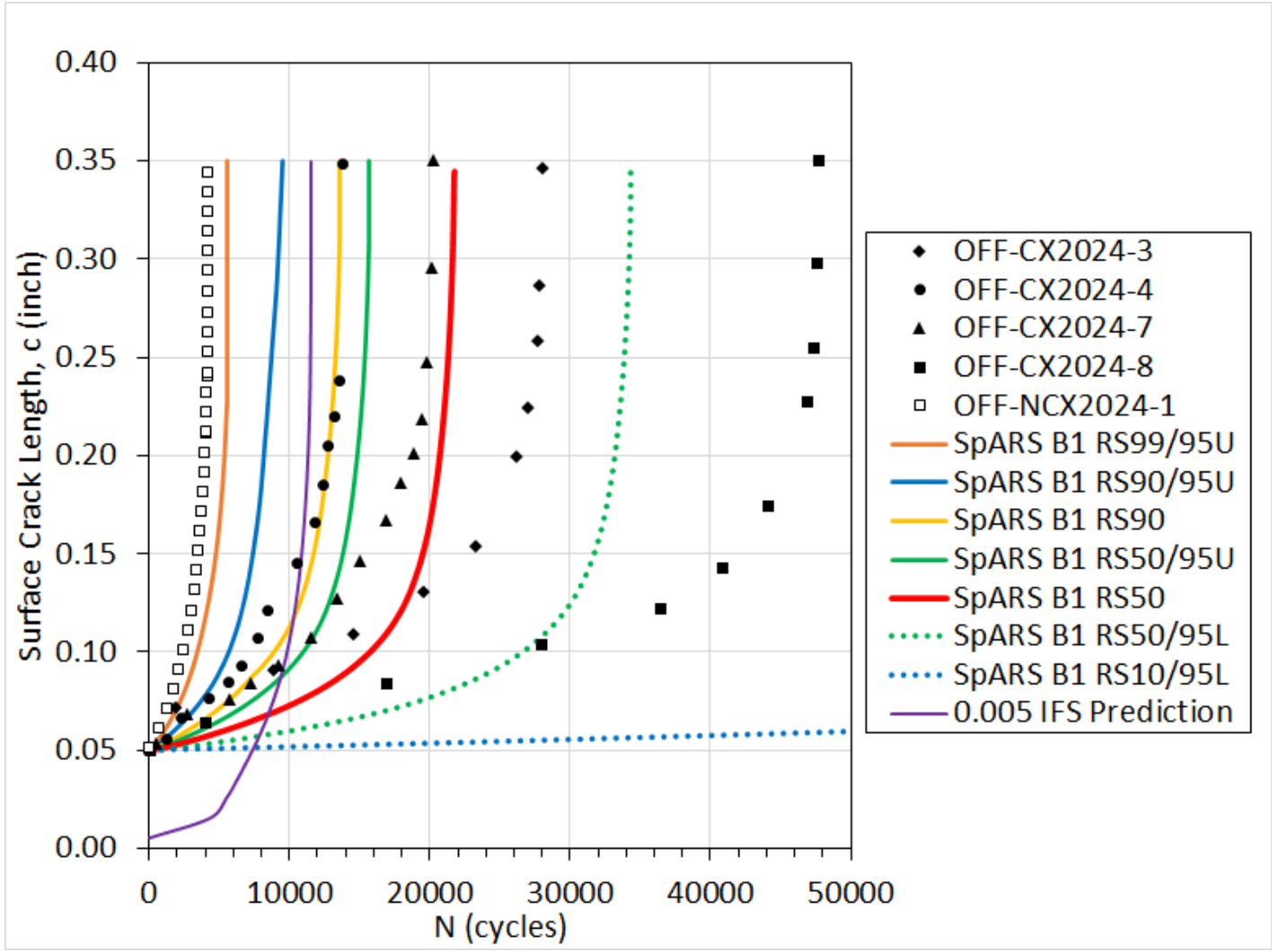

Summary

- Significant quantified benefits for predicting fatigue life and RII compared to legacy 0.005 inch approach
- Selected upper tolerance bound analysis prediction for these three case studies was $RS_{50/95U}$
  - Balances conservatism and safety, but with significant RII improvement

A2 Condition	Fatigue Life (normalized)	RII (normalized)
Non-Cx Test Data	1.0	1.0
Cx Test Data (2 reps)	25.0-25.4	22.3-22.7
0.005 inch prediction	3.5	1.6
SpARS A2 $RS_{99/95U}$	2.9	2.9
SpARS A2 $RS_{90/95U}$	6.8	6.8
SpARS A2 RS_{90}	8.0	8.0
SpARS A2 $RS_{50/95U}$	19.9	19.9
SpARS A2 RS_{50}	28.4	28.4

E1 Condition	Fatigue Life (normalized)	RII (normalized)
Non-Cx Test Data	1.0	1.0
Cx Test Data (9 reps)	62.6-99.1	62.6-99.1
0.005 inch prediction	3.5	1.6
SpARS E1 $RS_{99/95U}$	1.2	1.2
SpARS E1 $RS_{90/95U}$	3.2	3.2
SpARS E1 RS_{90}	6.8	6.8
SpARS E1 $RS_{50/95U}$	16.1	16.1
SpARS E1 RS_{50}	39.9	39.9

B1 Condition	Fatigue Life (normalized)	RII (normalized)
Non-Cx Test Data	1.0	1.0
Cx Test Data (4 reps)	3.3-11.4	3.3-11.4
0.005 inch prediction	2.8	0.99
SpARS B1 $RS_{99/95U}$	1.3	1.3
SpARS B1 $RS_{90/95U}$	2.3	2.3
SpARS B1 RS_{90}	3.2	3.2
SpARS B1 $RS_{50/95U}$	3.7	3.7
SpARS B1 RS_{50}	5.2	5.2

Summary

- There is an infinite number of possible tolerance bounds to utilize (for any combination of population quantile and confidence)
  - Typical aerospace-related bounds involve A- and B-basis representations ($RS_{99/95U}$, $RS_{90/95U}$)
- These statistical bounds quantify the uncertainty from
  - Tolerances in Cx process specification (hole D, mandrel D, sleeve t)
  - Inherent material variability
  - Uncertainty associated with the RS characterization method
  - SpARS model error

CONCLUSIONS

Conclusions

- This method addresses part of the need of USAF Aircraft Structural Integrity Program (ASIP) draft guidance currently under development
  - That guidance dictates "*multiple residual stress field characterizations must be used to generate a statistical representation that quantifies the cold expansion process and material uncertainties and variability, with the less compressive 95% upper bound statistical representation of the residual stress field to be utilized in all crack growth analyses utilized for fleet management*"
- This is an important step towards allowing an ASIP manager to safely and conservatively utilize known and quantified residual stresses in analyses to better manage their fleet and provide more aircraft availability with fewer inspections

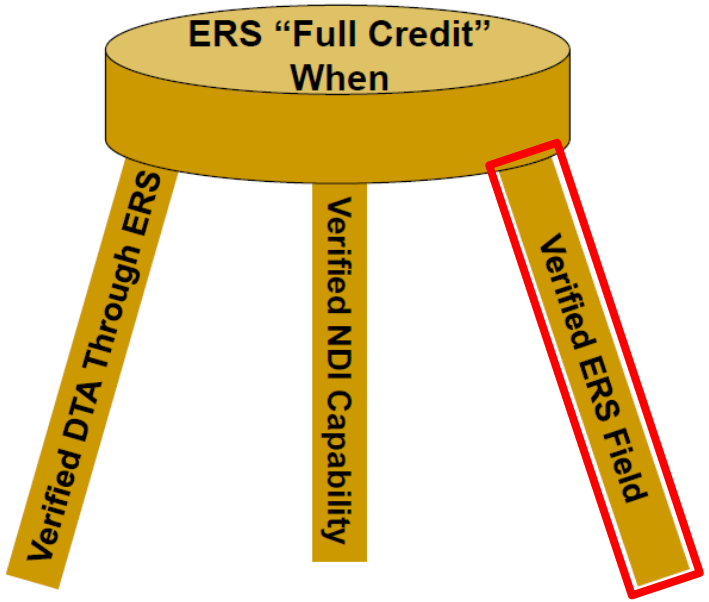

[6]

FUTURE WORK

Future Work

- Capability for accounting for the cracked body RS states
- Ensure allowable residual stress fields meet physical constraint requirement of static equilibrium
- Include measurement uncertainty of the RS data
- Address discrepancies between predictions and fatigue test data
- Perform probabilistic damage tolerance analysis and risk assessment
- Evaluate additional cases
  - Further validate the model and verify method
  - Identify the tolerance bound RS field selected for fleet management and establish practical guidelines

References

1. Pilarczyk RT. *Beta corrections to predict fatigue crack growth at cold expanded holes in 7075-T651 aluminum alloy* [MS Thesis]. Salt Lake City: Mechanical Engineering, University of Utah; 2008.

2. Andrew DL, Clark PN, Hoeppner DW. Investigation of cold expansion of short edge margin holes with pre-existing cracks in 2024-T351 aluminum alloy. *Fatigue Fract Eng Mater Struct.* 2014;37(4):406-416.

3. Tobler W. A computer movie simulating urban growth in the Detroit region. *Econ Geogr.* 1970;46, Supplement:234-240.

4. Jackson J. Definition of Design Allowables for Aerospace Metallic Materials. Paper presented at: AeroMat, 2007. https://www.mmpds.org/wpcontent/uploads/2015/03/mmpds_2015_2007aeromat_presentation.pdf.

5. Andrew, DL, Han, H-C, Ocampo, J, Alaeddini, A, Thomsen, M. Characterization of residual stresses from cold expansion using spatial statistics. Fatigue Fract Eng Mater Struct. 2020; 1– 14. https://doi.org/10.1111/ffe.13334

6. Babish C. ASIP Perspective on Accounting for Engineered Residual Stress in Damage Tolerance Analysis. Paper presented at: Aircraft Structural Integrity Program Conference. 2017; Jacksonville, FL.

utsa.edu